Meiotic mapping of radiation-induced DNA repair mutations and aberrations in *Aspergillus nidulans*: special features and use of translocations

E. Käfer - Institute of Molecular Biology and Biochemistry, Simon Fraser University, Burnaby, B.C., Canada, V5A 1S6

We recently described epistatic grouping of several new DNA repair genes and reported their location in the genetic map of Aspergillus (Fig. 1 in Käfer and Chae 1994 Curr. Genet. 25:223-232 and next report in this Newsletter). Some of the properties of the 10 mutations involved are listed in Table 1. Supporting mapping data are presented here which showed the following special features; unusual patterns of recombination which identified three types of radiation-induced aberrations; useful translocation breaks some of which link up fragments of the meiotic map and will provided new markers for a physical map of the long arm of chromosome VII; poorly-fertile mutants which in heterozygous crosses produced "twin" cleistothecia, partly selfed for the other normally self-sterile parent; aberration-free strains which produced consistent recombination frequencies without chiasma interference, possibly because they were practically isogenic.

The origin and isolation of the mapped mutations have been reported years ago, *musK* - *musS* by Käfer and Mayor (1986 Mutat. Res. 161:119-134) and *uvsI* by Han et al. [1983 Korean J. Env. Mut. Carcin. 3:21-33]. To obtain null mutations caused by chromosome breaks, the mutagen-sensitive mutants had been induced by high doses of radiation (5-15% survival). About two aberrations per survivor had been identified in the original *mus* strains, but it is now clear that only 7 aberrations were induced by radiation in the 10 strains analyzed (Table 1). A spontaneous I;III translocation was found in the strain used for isolation of mutants (FGSC #A605) as confirmed in pulsed field gels (Brody et al. 1991 Nucl. Acids Res. 19:3105-3109). The translocation breaks of this spontaneous T2(I;III) were mapped on the left arms of chromsomes I and III (Fig. 1) which complicated the mapping of mutations on these chromosomes. Strains of the 10 mapped DNA repair mutations with useful markers are now available, 6 of them translocation-free and 4 associated with an aberration (FGSC A828, A838, and A840-847).

For general mapping of mus mutations and aberrations, mitotic analysis of heterozygous diploids was combined with testing of random ascospore progeny, including aneuploids and duplications from heterozygous translocation crosses (Käfer 1977 Adv. Genet. 19:33-131). In brief, suitable segregants from the original mapping diploids were crossed repeatedly to standard strains with potentially linked markers (translocation-free segregants of *musK, N*, and *uvsI* for 2-4 generations, and all others for 8 or more). Recombinants were checked for translocations by testing haploids from heterozygous diploids for inter-chromosomal linkages or by monitoring crosses for increased aneuploid frequencies. In this way either translocation-free progeny were obtained or associated aberrations identified. For the latter cases, chromosome breaks were

located to chromosome segments using homozygous diploids and mutations were mapped by meiotic linkage to markers on the two chromosomes involved.

Table 1. Genetic analysis of radiation-induced DNA repair-deficient mutations

Map location[1], induced aberrations, fertility, and effects on mitotic recombination[2]

Genes and allele Nos	Map location Chromosome arm	Assoc. trans-location[3]	Closest markers	Other γ-ray induced aberrations	Fertility in homozygous crosses	Level of mitotic recombination
γ-ray-induced *mus* and aberrations [in FGSC A605: *biA1 T2(I;III); AcrA1; nicA2*]						
musK228	*VIIIR*	none	*nirA*	none	normal	reduced
musL222	*IR*	none	*biA*	*T(II;VIII)*	sterile	eliminated
musM225	*VIR*	*Ab(VI.2)*	*sbA?*	none	normal	not tested
musN227	*VIIR*	none	*choA*	none	sterile	increased
musO226	*IIIL / VIIR*	*T2(III;VII)*	*meaB*	none	sterile	allelic high
musQ230	*IIR*	none	*adC*	*T(III;VII;VIII)*	sterile	increased
musR223	*IIIL*	none	*dilA*	*T(I/III;VI)*	normal	normal
musS224	*IIIL / VIIR*	*T3(III;VII)*	*actA/ pantoB*	none	normal	normal
UV- induced *mus* and aberration (in FGSC A610: *pabaA1 yA2*)						
musP234	*IIL / VIIR*	*T2(II-VII)*	*malA*	none	sterile	normal
UV-induced *uvsI* (in FGSC A168: *suA1adE20 adE20 biA1; ssbA1; sB3; choA1; chaA1*)						
uvsI501	*IIIL*[4]	none	*sA*	none	normal[4]	normal[4]

1 For overview maps see Käfer and Chae (1994 Curr. Genet. **25**:223-232) or the map of Aspergillus compiled by Clutterbuck (1994 Catalogue of Strains, FGSC 5th ed., 1993 in "Genetic Maps" O'Brien ed. 6th ed. vol 3:71-84, Cold Spring Harbor Lab. CSH NY).

2 From Zhao and Käfer 1992 (Genetics **130**:717-728)

3 For *mus O*, *P* and *S* the location of the wild type gene at one of the two translocation breaks has not yet been identified

4 Chae 1993 (PhD thesis McGill University, Montreal); Chae and Käfer 1993 (Curr. Genet. **24**:67-74)

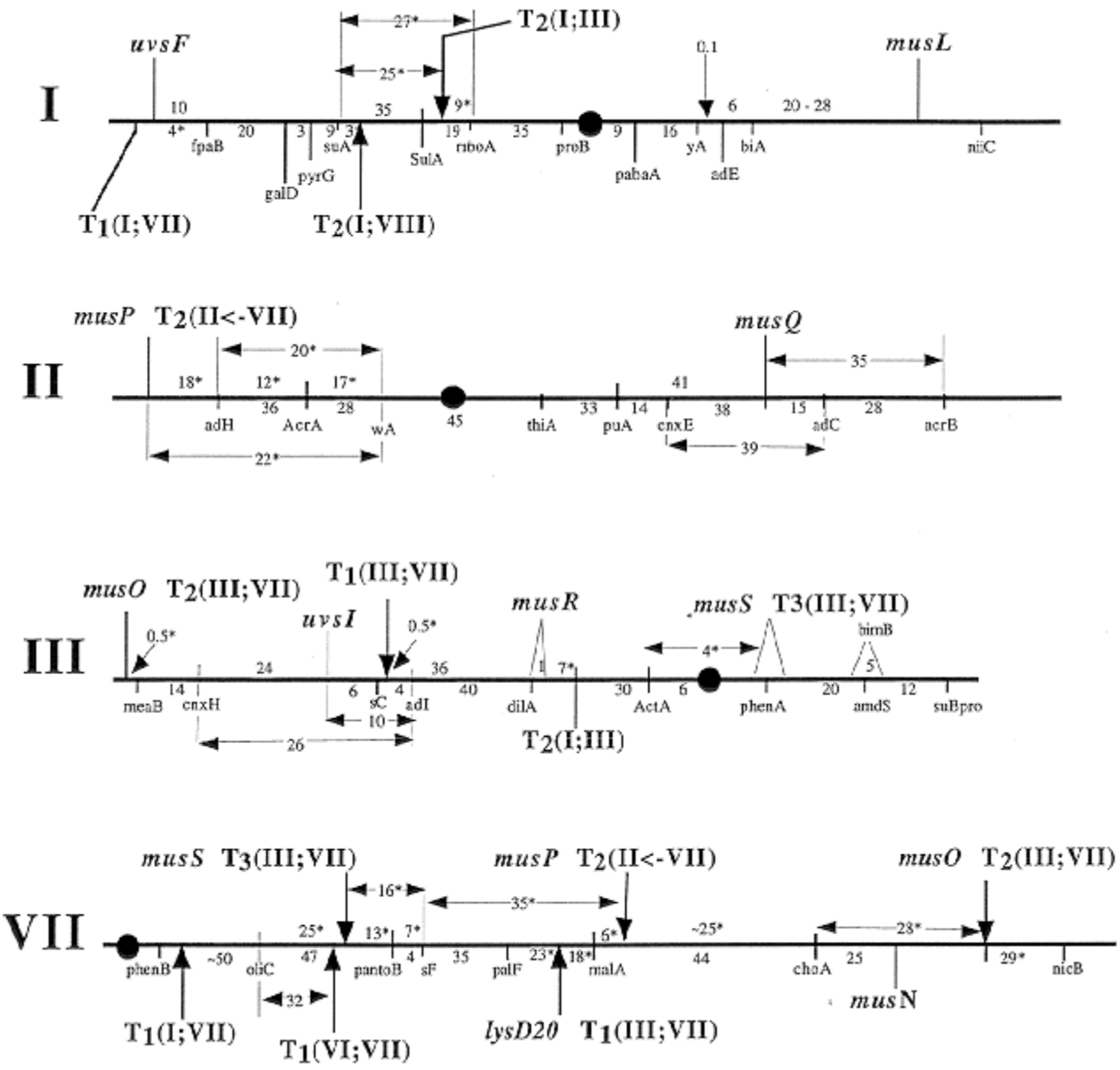

Fig 1. Map location of new DNA repair genes and associated translocations in linkage groups I to III and VII of A. nidulans (Table 1; *musK* of LG VIII, and *musM* of group VI, are not shown). Numbers represent recombination frequencies in percent, asterisks (*) indicate reduced crossover values from heterozygous translocation crosses (for gene symbols, see Clutterbuck 1993 ref. cit.).

Figs 2 - 4. Detailed linkage maps of mus mutations associated with translocations. Recombination frequencies for inter- and intra-chromosomal linkages in heterozygous crosses are indicated; these are reduced compared to standard map values (Fig. 1).

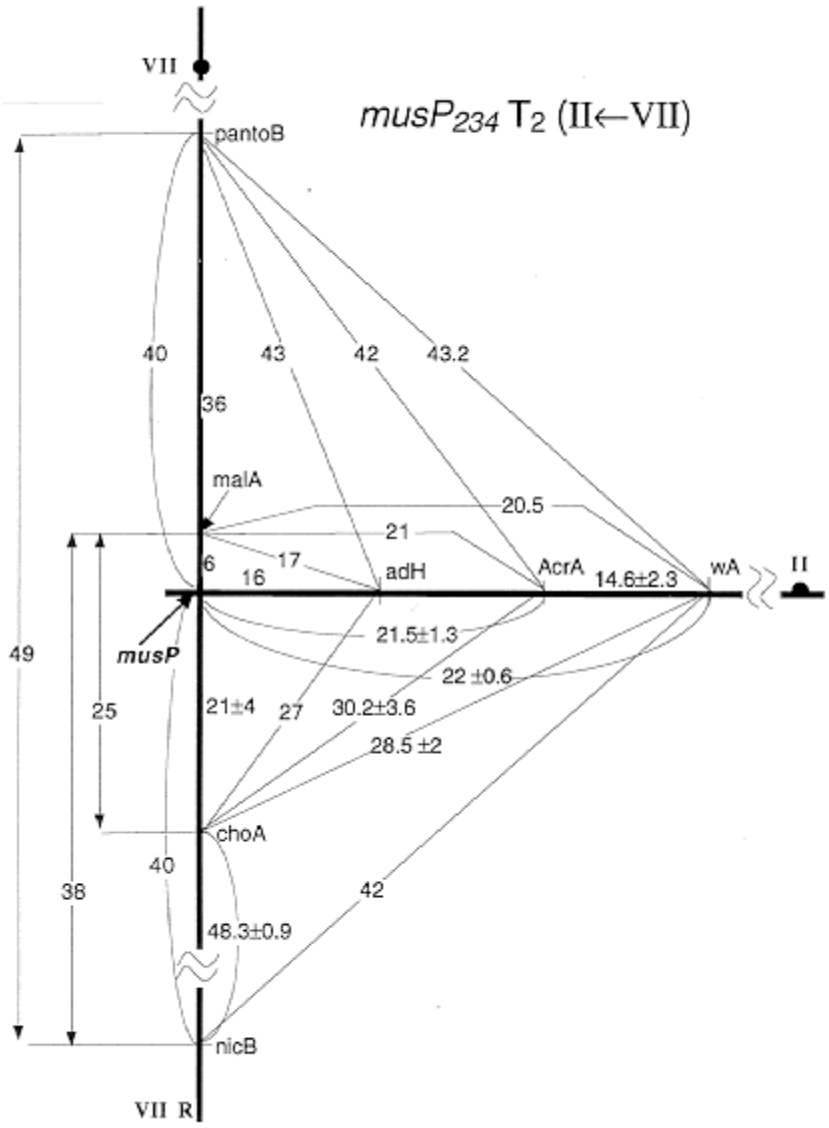

Fig 2: musP mapped at the break points of the unidirectional T2(II<-VII);

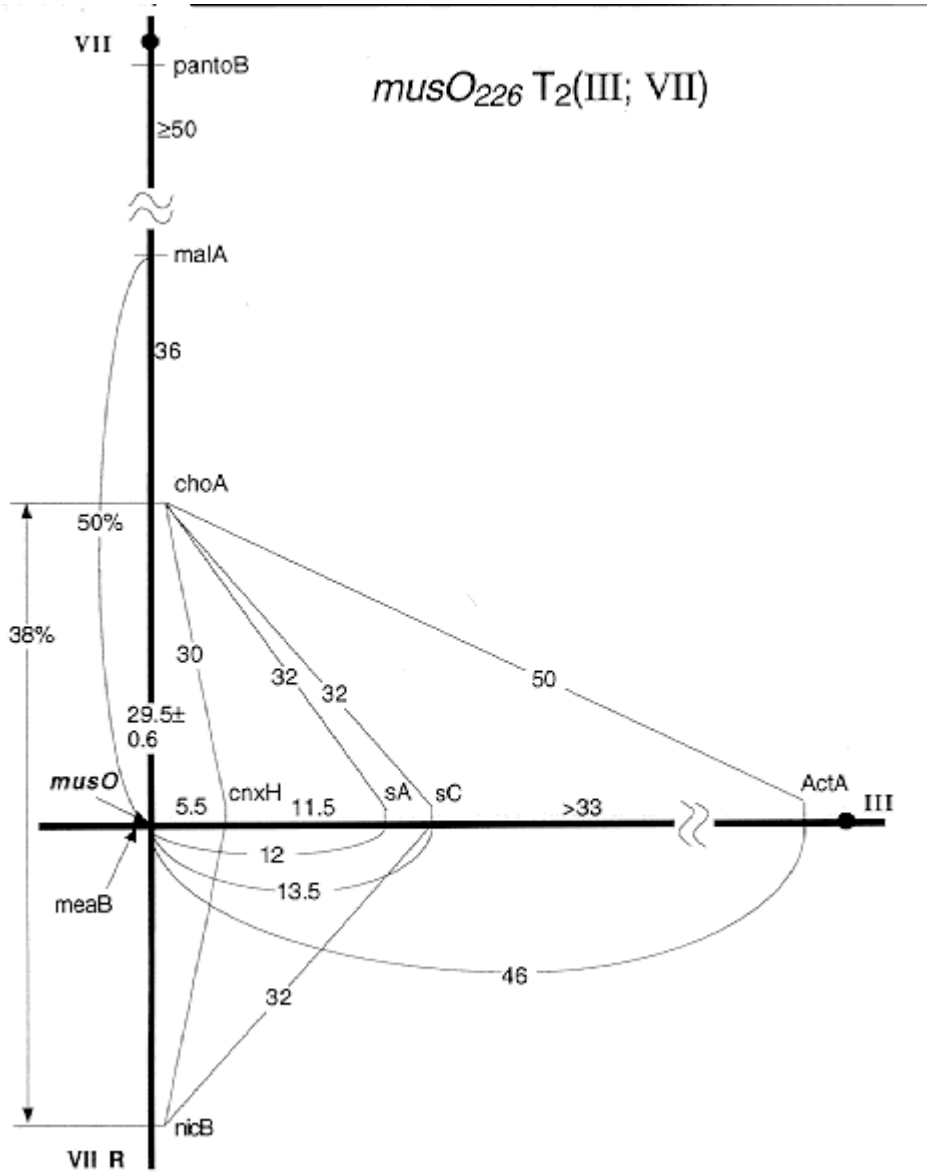

Fig 3: musO T2(III:VII) with distal break points on the chromosome arms of IIIL and VIIR

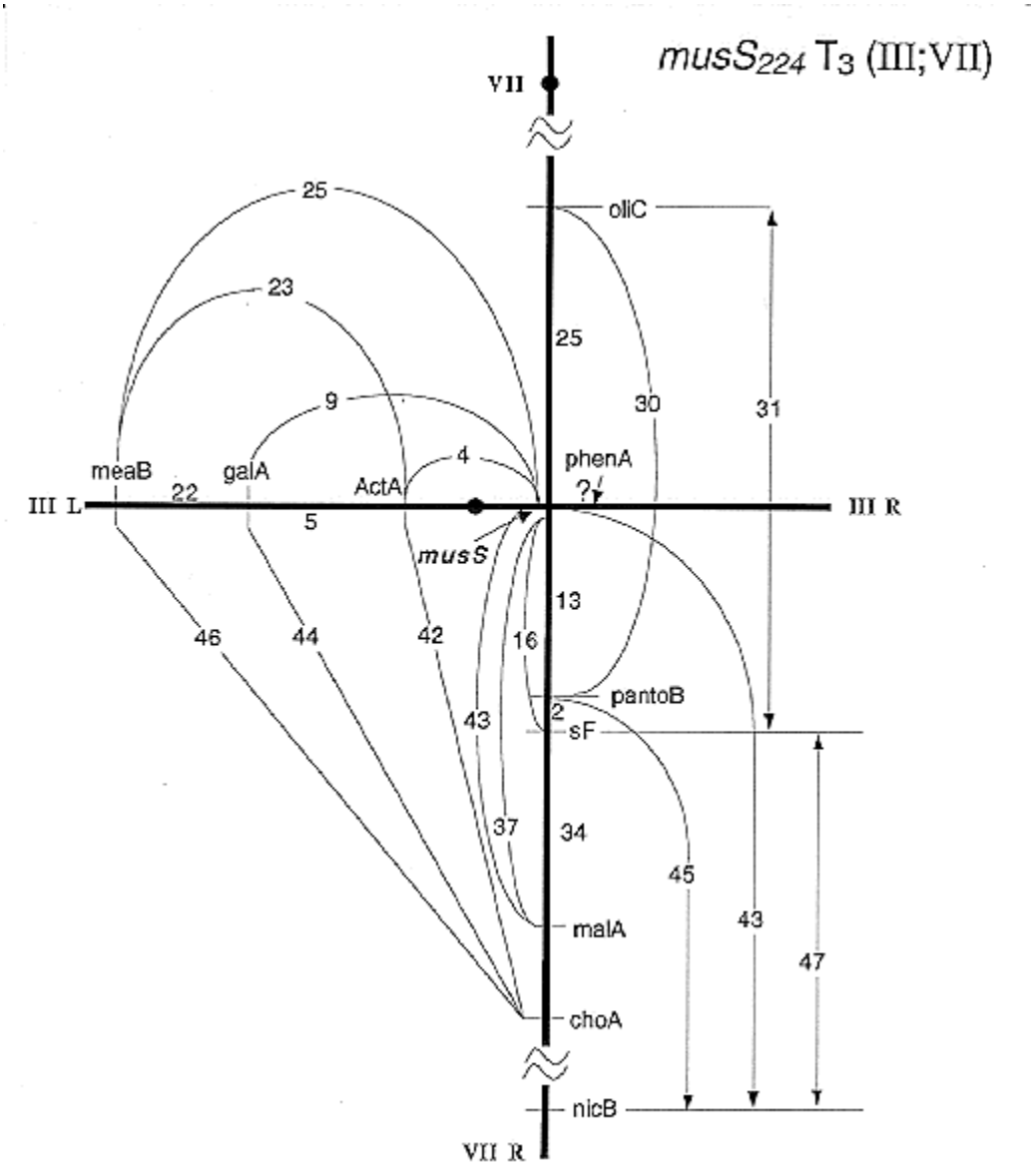

Fig 4: musS mapping proximal on IIIR and VIIR.

Results for musM suggested that this MMS-sensitive mutation was associated with an intra-chromosomal aberration. It clearly was located on chromosome VI but showed meiotic linkage with all markers of this linkage group (LG) VI even with 3 unlinked ones (*bwA, sB* and *sbA*). Associated translocations were identified in 3 other cases, *musP, O*, and *S* (Table 1). The respective mutations showed meiotic linkage to markers of two linkage groups (Fig. 1) and it is not known in which of the two chromosomes the gene is located. In the case of *musP234*, the translocation was found to be unidirectional [T2(IIL<-VIIR); Fig. 2]. No duplication segregants were seen among haploids from *musP*/+ diploids, but in low-density platings of ascospores about 30% of colonies were probably duplications. They produced sectors which segregated for markers of the distal half of VIIR (*choA* and *nicB*). This finding and the map location of the translocation breaks (distal on IIL and in the middle of VIIR; Fig. 2) are consistent with a unidirectional T2(IIL<-VIIR). Two other cases were reciprocal translocations between

chromosomes III and VII. The breaks of *musO226* T2(III;VII) mapped fairly distal, especially on VIIR where *musO* was located in the most distal gap of the meiotic map of LG VI (Fig. 3). In contrast, *musS224* T3(III;VII) mapped closer to the centromere, especially on IIIR, as identified in homozygous diploids (Fig. 4).

The map location of all other mus mutations is based on the data of Tables 2-7. In these final aberration-free crosses, linkage values were very consistent and agreed well with previously published ones. Average recombination frequencies between all possible pairs of markers are presented for 4 cases, *musK, R, Q*, and *L* (Tables 2-5) and in 2 of them raw data for one cross are shown as well. Mutations could be located unambiguously in most cases; e.g., *musK228* was mapped distal to all markers in LG VIIIR, based on practically identical results from 2 crosses which showed good additivity (Table 2). Only the location of *musR223*, very close distal or proximal of *dilA*, is not yet known exactly, even though standard errors were small and linked aberrations had been eliminated (Fig. 1; Table 3); because only fairly distant other markers segregated in the cross to *dilA*, single and double crossovers were equally frequent. Similarly, results were ambiguous in the first mapping cross of *musQ* in which results suggested a position distal to *adC* (evident in cross 2284; Table 4). However, crosses with the additional marker *acrB* clearly placed it proximal to adC (Fig. 1). Results for *musL* were complicated in early crosses by linkage to the spontaneous translocation T2(I;III), and in general by poor viability and recovery of *musL*. Among ascospores, the frequency of *musL* was about 15%, but in recorded results allele ratios were usually higher, because the poorly-growing musL progeny tended to be isolated preferentially (Table 5). In addition, fertility of *musL* was very poor in heterozygous crosses [e.g., crosses to more distal markers were not successful]. This presumably caused the observed unusual production of "twin-type" cleistothecia; i.e., a mixture of 2 sets of ascospores, one of them hybrid and segregating for *musL*, the other consisting of selfed progeny of the second parental strain. These problems made accurate location of *musL* distal to *yA* and *biA* impossible.

When the patterns of double or triple crossing over were analyzed, almost complete absence of chiasma interference was evident in all crosses; e.g., one class of the single crossover (CO) types was often less or equally frequent as the corresponding double CO types. This suggests random distribution of chiasmata without interference, as evident in the crosses of uvsI (Table 7). The data from *musN* crosses with more distant markers are less conclusive (Table 6) because in such crosses interference is diminished in all species (Foss et al. 1993 Genetics 133:681-891).

In summary, meiotic mapping revealed that in 4 cases radiation-induced aberrations were associated with mus mutations which presumably are null-mutations. Three types of aberrations were identified: an inversion, a unidirectional translocation, and two reciprocal translocations. Such aberrations reduce meiotic recombination frequencies in heterozygous crosses and are exploited for genetic mapping in various species. The postulated inversion *musM225* (AbVI-2) is not yet mapped well enough to be used in this way. It resembles the known inversion, *lysA1* (AbVI-1) located in the same LG, which can be detected by high aneuploid frequencies in crosses to overlapping translocations. On the other hand, three translocations that have been mapped will be useful. The unidirectional translocation of *musP234* transfers the distal half of the right arm of chromosome VII to the tip of IIL. When crossed to mutations assigned to LG VII, these will be disomic in the resulting duplications only if they are located distal to the break point (near *malA*). However, it will be important that progeny from such crosses not be used for

standard analysis, since in this case duplications and their sectors are not verydistinct and near-haploid products from duplications may accumulate further aberrations (Roper and Nga 1969 Genet. Res. 14:127-136). Two reciprocal translocations both involve chromosomes III and VII. One of them, *musS223* T3(III;VII), will be a useful centromere marker on IIIR, while the other, *musO226* T2(III;VII), provides meiotic linkage between *choA* and *nicB*, connecting the most distal segments of VIIR (Fig. 1). This should make it possible to orient the markers of the *nicB* fragment (as recently achieved for the distal IIR region in fission yeast; Egel 1993 Curr. Genet. 24:179-180). Several previous translocations were mapped in LG VII and these were essential for the mapping of the centromere and the ordering of 7 meiotically unlinked fragments (Käfer 1977, ref. cit.). Even now the standard meiotic map of linkage group VII has 6 gaps with 40-50 % recombination and translocation breaks have so far been placed into only 3 such gaps; therefore 3 gaps without linkage remain in the meiotic map of VIIR.

The location of all *mus* mutations which were separable from aberrations could be identified accurately, except for *musL*. Recombination between *musL* and *yA* or *biA* varied widely among progeny of different color, because samples were non-random for *musL* as well as *yA*. In addition, mapping was inaccurate because "twin" cleistothecia were frequent (as found also for other poorly fertile mutations; e.g., *bimD*; Denison et al. 1993 Genetics 134:1085-1096). Such twins were "dizygotic" and contained selfed ascospores of the other parent, even if this strain was normally self-sterile (e.g., *ribo*-). It seems likely that in these crosses fertility is increased by cross-complementation. The partial selfing further increased the uncertainty of linkage values even when several unlinked markers segregated and purely parental types, could be identified.

Aberrations or mutations which reduce recombination and reveal meiotic linkages are especially helpful in species with genetically large chromosomes; i.e., not only for our standard strains which are all derived from backcrossed strains that originated from a single nucleus (Pontecorvo et al. 1953 Adv. Genet. 5:141-232) but also for strains of fission yeast which had a similar origin. In this yeast, as in *A. nidulans*, recombination values are large and practically without interference and long-range mapping requires special recombination-defective strains (Schmidt 1993 Curr. Genet. 24:271-273). In both species strains are therefore isogenic barring induced mutations. In contrast, species which show chiasma interference, such as Neurospora or Drosophila, depend on crosses of less closely related strains of opposite mating type or sex. High recombination without interference may therefore be related to isogenicity, especially since highly backcrossed strains of *N. crassa* consistently showed higher recombination and less interference (Käfer 1982 Neurospora Newsl. 29:41-44). Evidnce for or against this hypothesis is starting to accumulate as techniques are becoming available for measurements of divergence at the nucleotide level and in some cases effects of heterology on recombination and on related processes have been demonstrated (e.g., Resnick et al. 1989 PNAS 86:2276-2280).

Acknowledgement: This work was supported by a grant from the Natural Sciences and Engineering Research Council of Canada.

Table 2: Mapping of *musK* in linkage group VIII

Recombination between relevant markers from 2 similar crosses

Cross No.	Relevant genotypes					Totals tested
(2638)	*musK228*	x	*chaA1*	*sE15*	*nirA14*	: 108
(2738)	*musK228*	x *riboB2*	*chaA1*	*sE15*		: 165
				Combined		: 273

% (percent in bold): Average % between *musK* and markers at increasing distance
Diagonal: CO (in percent) between adjacent markers
No = Sum of CO types from one or both crosses / Total

Markers	*riboB*		*chaA*		*sE*		*nirA*	
	%	No	%	No	%	No	%	No
musK	**50.9**	84/165	**29.1**	28+41/273	**22.3**	24+37/273	**12.0**	13/108
nirA	—		18.5	20/108	10.2	11/108	—	
sE	50.9	84/165	14.7	16+24/273	—			
chaA	50.9	84/165	—					

Table 3: Mapping of *musR* in linkage group III

Recombination between relevant markers from 3 crosses

Cross No.	Relevant genotypes						Totals tested
(2239)	*musR223*	x	*galE9*	*meaB6*	*adI50*		: 232
(2998)	*musR223*	x		*meaB6*	*adI50*		: 159
(2999)	*dilA1*	x		*meaB6*	*adI50*	*musR223*	: 168
						Total	: 559

% (percent in bold): Average % between *musR* and markers at increasing distance
Diagonal: CO (in percent) between adjacent markers
For marker pairs common to all crosses, averages and their standard errors are shown.

Markers	*galE*	*meaB*	*adI*	*dilA*
	%	% (±SE)	% (±SE)	%
musR	**44**	**41.9** (± 0.3)	**38.2** (± 1.2)	**1.2**
dilA	—	42.3	41.7	—
adI	37	33.2 (± 1.3)	—	
meaB	20	—		

Table 4: Mapping of *musQ* in Linkage group II

Recombination between relevant markers from 3 crosses:

Cross No:	Genotypes	Total tested
(2774)	*musQ230* x *wA3* *cnxE16*	: 139
(2284)	*musQ230* x *wA3* *puA1* *cnxE16* *adC1*	: 229
(2285)	*musQ230* x *wA3* *puA1* *cnxE16* *adC1* *acrB2*	: 240
		608

Upper left of table: Results of one cross (2284), Nos. of 4 types of progeny shown: $\frac{\text{(2 CO-types)}}{\text{(2 P-types)}}$

Lower right of table: Average percent recombination of the 3 crosses combined

% (percent in bold): Average % between *musQ* and other markers

Markers Cross (2284)	*wA* %	*wA* No	*puA* %	*puA* No	*cnxE* %	*cnxE* No	*adC* %	*adC* No		----	*acrB*
musQ	46	49+57 / 71+52	40	51+40 / 89+49	38	47+39 / 90+53	15	16+19 / 110+84	----	28 %	*adC*
adC	45	48+54 / 72+55	39	52+38 / 88+51	35	46+34 / 92+59	----		**15 %**	**35 %**	***musQ***
cnxE	51	49+68 / 70+42	11	14+12 / 126+77	----		**38 %**		39 %	46 %	*cnxE*
puA	49	46+66 / 74+43	----		12 %		**41 %**		38 %	44 %	*puA*
	----		48 %		49 %		**44 %**		47 %	51 %	*wA*
Map distances	*wA* % 48		*puA* 12		*cnxE* 38		***musQ*** ***15***		*adC* 28	*acrB*	

Table 5: Mapping of *musL* in linkage group I

Recombination between relevant markers from 3 crosses:

Cross No:	Genotypes				Total tested
(2672)	*T2(I;III) musL222*	x	*pabaA1 yA2 biA1;(fwA2)*	:	160
(2922)	*SulA1 musL222*	x	*anA1 pabaA1 yA2biA1*	:	150*
(2923)	*yA2 musL222; (fwA2)*	x	*SulA1*	:	102

Upper left of table: Results of one cross (2922), numbers of 4 types of progeny shown: $\frac{\text{(2 CO-types)}}{\text{(2 P-types)}}$

Lower right of table: Average percent recombination of the 3 crosses combined;
% (percent in bold): Average % between *musL* and markers at increasing distance
Diagonal: CO (in percent) between adjacent markers

Markers (Cross: 2922)	*SulA* %	*SulA* No	*anA* %	*anA* No	*pabaA* %	*pabaA* No	*yA* %	*yA* No	*biA* %	*biA* No	***musL*** **%**
musL	57	$\frac{20+65}{21+44}$	40	$\frac{22+38}{19+71}$	20	$\frac{13+17}{28+92}$	15	$\frac{14*+8}{27+101}$	15	$\frac{14*+8}{27+101}$	—
biA	43	$\frac{18+46}{17+69}$	35	$\frac{15+37}{20+78}$	12	$\frac{4+14}{27+101}$	4	$\frac{3+3}{29+115}$		—	**18**
yA	40	$\frac{16+44}{19+71}$	33	$\frac{14+36}{21+79}$	9	$\frac{2+11}{32+105}$		—		4.5	**20**
pabaA	37	$\frac{19+37}{26+68}$	29	$\frac{16+28}{29+77}$		—		10		11	**24**
anA	21	$\frac{22+38}{19+71}$		—		29		33		35	**40**
SulA		—		21		37		39		40	**47**

* Non-random sample, enriched for *musL222* and *yA* progeny

Table 6. Crossing over of *musN* with markers of linkage group VII

Cross 2737 **Types** of recombinants	**Markers -> crossover intervals** *malA* (1) *choA* (2) *musN* (3) *nicB*								**Progeny** No	Percent
Parental -1	+		+		-		+		9	P1 + P2
P-2	-		-		+		-		9	18.9 %
Single CO	+		-		+		-		7	
interval (1)	-	X	+		-		+		5	12.6 %
Single CO	+		+		+		-		3	
interval (2)	-		-	X	-		+		1	4.2 %
Single CO	+		+		-		-		17	
interval (3)	-		-		+	X	+		9	27.4 %
Double CO	+		-		-		+		3	
Int. (1+2)	-	X	+	X	+		-		0	3.2 %
Double CO	+		-		+		+		11	
Int. (1+3)	-	X	+		-	X	-		4	15.8 %
Double CO	+		+		+		+		9	
Int. (2+3)	-		-	X	-	X	-		2	11.6 %
Triple CO	+		-		-		-		4	
Int. (1+2+3)	-	X	+	X	+	X	+		2	6.3 %
Adjacent intervals CO: No	*malA* - *choA*		36	*choA* - *musN*	24	*musN* - *nicB*	58		(95)	Total
%			**37.9**		**25.3**		**61.1**			
Crossover frequencies in other intervals (No) %	*malA* ----- *musN* (42) **44**									
	choA ---- *nicB* (48) **50**									

Table 7. Crossing over between *uvsI* and markers of linkage group III

Cross No.	Crossover types	Markers									Progeny		
		cnxH		*uvsI*		*sC*		*adI*		*methH*	No. and sum of reciprocals		Percent
3019	**Parental**-1	-		+		-					64		
	P-2	+		-		+					48	112	73 %
	Single CO	-		-		+					14		
	distal	+	X	+		-					18	32	21 %
	Single CO	-		+		+					2		
	proximal	+		-	X	-					3	5	3 %
	Double	-		-		-					2		
	CO	+	X	+	X	+					2	4	2.5 %
	Total No		36		9							153	
	CO %		24		6								
3020	**Parental**-1			+				-		-	47		
	P-2			-				+		+	61	108	54 %
	Single CO			+				+		+	6		
	distal			-		X		-		-	5	11	5.5 %
	Single CO			+				-		+	36		
	proximal			-				+	X	-	37	73	36 %
	Double			+				+		-	5		
	CO			-		X		-	X	+	5	10	5 %
	Total No					21		83				202	
	CO %					**10**		**41**					
3019 + 3020	Meiotic map of *uvsI* in %	*cnxH* -	**24**	*uvsI* -	**6**	*sC* -	**4**	*adI* -	**41**	*methH*			